THE JOURNAL OF PHYSICAL CHEMISTRY B

Article

pubs.acs.org/JPCB

Computational Investigation of the Initial Two-Electron, Two-Proton Steps in the Reaction Mechanism of Hydroxylamine Oxidoreductase

Amr A. A. Attia and Radu Silaghi-Dumitrescu*

Department of Chemistry, Babes-Bolyai University, Cluj-Napoca, RO-400028 Romania

Supporting Information

ABSTRACT: Reported here is a computational study based on density functional theory that presents the first attempt to investigate the 2-electron 2-proton reaction of Fe(III)−H_2NOH to Fe(III)−HNO in the catalytic cycle of hydroxylamine oxidoreductase—a multiheme-containing enzyme that catalyzes the conversion of hydroxylamine (HA) to nitrite in nitrifying bacteria. Two subsequent protonation events are proposed to initiate the process, of which the second is suggested to be concerted with a one-electron oxidation. The final one-electron oxidation is further proposed to be accompanied by a third deprotonation process, suggesting that Fe(III)−HNO may not be an isolable intermediate in the HAO catalytic cycle. Further explorations are suggested to be focused on the following steps in the catalytic cycle, the influence of the lateral substituents of the heme (and especially of the Cys and Tyr cross-links), the comparative study of hydrazine oxidation, the proton delivery network in the distal site and, possibly, on linkage isomerism.

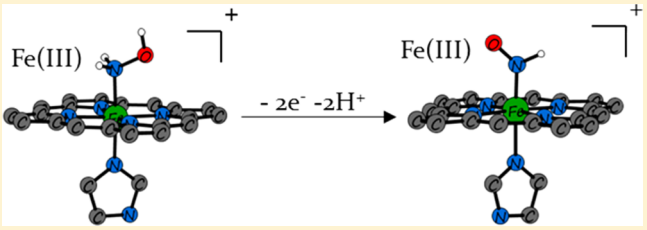

INTRODUCTION

Hydroxylamine oxidoreductase (HAO) is a multiheme-containing enzyme that catalyzes the four-electron oxidation of hydroxylamine (HA) to nitrite in nitrifying bacteria.[1] HAO is a complex homotrimer hosting a total number of 24 heme units. Each monomer comprises seven *c*-type heme units and an eighth P460 heme. The P460 heme is pentacoordinated with an axial His ligand and an unoccupied sixth coordination site where the binding and oxidation of HA takes place. The remaining seven *c*-type hemes are all hexacoordinated, each with two axial His ligands, in the expected low spin states, and disposed in space as an optimized chain of electron transfer.[2−4]

The generally accepted catalytic cycle of HAO starts off with the aqua-bound ferric P460 heme, which is the proposed resting state. HA is then introduced replacing the water molecule to form a HA-bound ferric heme structure, which then proceeds by losing two protons and two electrons to yield a nitroxyl (HNO) bound heme in the ferric state. A subsequent loss of a proton leaves a state of equilibrium between a ferric heme bound to a nitroxyl anion and a ferrous state bound to NO, that is, $\{FeNO\}^7$ in Enemark−Feltham notation.[5] A loss of an electron then follows to form $\{FeNO\}^6$, which may be regarded as an equilibrium state between a ferric heme bound to a nitric oxide and a ferrous heme bound to a nitrosonium ion. A water molecule is then introduced to the active site condensing the nitrosonium ion and yielding a nitrite-bound ferrous P460 heme. Nitrite then dissociates also liberating an electron and a proton, all followed by the binding of a water molecule to regenerate the proposed resting aqua ferric state.[2−4]

The formation of the NO intermediates $\{FeNO\}^7$ and $\{FeNO\}^6$ in HAO is still under active debate. Previously, studies have suggested that the oxidation of HNO to HNO_2 is a two-electron step where an NO would not be an intermediate.[6,7] However, recent studies have shown that NO is confirmed as an intermediate in the catalytic cycle of HAO, though not a long-lived one.[8−14] Moreover, a recent computational study on HAO by Fernandez and co-workers was reported that focused on the covalent linkage between a tyrosyl residue of one subunit and a mesocarbon atom of the heme active site of another subunit in HAO, and on the influence of this bond on the enzyme catalysis. Their results indicate that the tyrosine residue enhances the binding of hydroxylamine and increases the stability of a Fe(III)−NO intermediate, while having little effect on the Fe(II)−NO form.[15]

While many studies have been reported focusing on the NO intermediates of HAO, no attempt has been made to investigate the 2-electron 2-proton reaction of Fe(III)−H_2NOH to Fe(III)−HNO, which constitutes the first series of steps in the catalytic cycle. The exact sequence by which electrons and protons are lost is yet to be established. In this study, we carry out a theoretical investigation based on density functional theory that provides a detailed account of these steps.

COMPUTATIONAL METHODS

The chemical structures investigated in this study are depicted in Figure 1. A model for the active site of HAO was constructed

Received: July 16, 2014
Revised: September 26, 2014

   dx.doi.org/10.1021/jp507023a | *J. Phys. Chem. B* XXXX, XXX, XXX−XXX

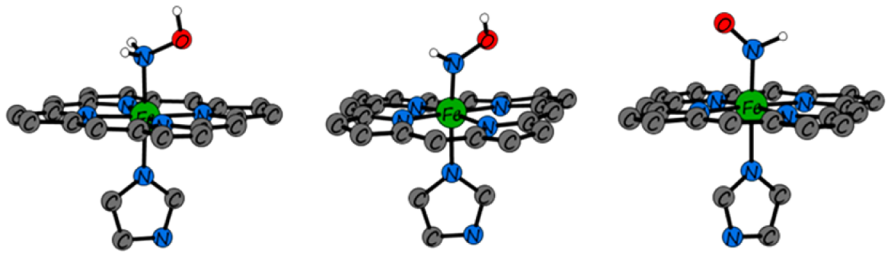

Figure 1. Models employed in the present study. Hydrogens of the porphine ring and the imidazole ligand of each structure are omitted for clarity.

Table 1. Relative Energies (kcal/mol), Bond Lengths (Å), Mulliken Atomic Charges, and Spin Densities of Fe(III)−H_2NOH

S	ΔE	Fe−N_{im}	Fe−N_{HA}	N−O	Fe spin	HA spin	Fe charge	HA charge
1/2	0.0	1.97	2.02	1.41	0.99	0.01	1.62	0.19
3/2	4.2	2.21	2.31	1.42	2.86	0.06	1.65	0.11
5/2	1.6	2.15	2.28	1.42	4.30	0.06	1.79	0.12

Table 2. Energies (hartree), Key Bond Lengths (Å), Mulliken Atomic Spin, And Charges for Models Examined in the Present Study. The Overall Charge on Each Model Is Shown in Square Brackets

	formal description	energy	Fe−N_{im}	Fe−N	N−O	Fe spin (charge)	ligand[a] spin (charge)
1	Fe(III)−H_2NOH [+1]	−2609.70564835	1.978	2.020	1.414	0.99 (1.62)	0.01 (0.19)
2	Fe(IV)−H_2NOH [+2]	−2609.34145130	1.977	2.031	1.416	0.00 (1.61)	0.00 (0.19)
3	Fe(II)−HNOH [0]	−2609.27945320	2.074	1.843	1.393	0.55 (1.53)	0.54 (−0.15)
4	Fe(III)−HNOH [+1]	−2609.06674565	2.006	1.759	1.352	0.00 (1.58)	0.00 (0.08)
5	Fe(V)−H_2NOH [+3]	−2608.88369683	1.972	2.055	1.412	−1.03 (1.65)	0.02 (0.23)
6	Fe(I)−HNO [−1]	−2608.71701946	2.102	1.813	1.249	−0.36 (1.41)	0.53 (−0.34)
7	Fe(IV)−HNOH [+2]	−2608.73065065	2.003	1.842	1.324	1.63 (0.81)	0.21 (−0.81)
8	Fe(II)−HNO [0]	−2608.68990376	2.085	1.781	1.228	0.00 (1.51)	0.00 (−0.19)
9	Fe(III)−HNO [+1]	−2608.49559400	2.052	1.843	1.212	1.27 (1.63)	−0.33 (−0.01)

[a]The axial ligand trans to imidazole be it H_2NOH, HNOH, or HNO.

comprising a heme without lateral substituents and an axial protonated imidazole as a model of histidine. The reactive intermediates were modeled by placing H_2NOH, HNOH, and HNO in the sixth coordination position trans to the imidazole.

The present theoretical investigation is based on density functional theory (DFT) utilizing the Gaussian 09 suite of programs[16] and Gauss view as front-end.[17] The meta GGA M06-L functional[18] was employed in all calculations coupled with the triple ζ 6-311+G(d,p) basis set. We point out that the M06-L functional was designed to include medium-range electron correlation effects (which is usually what is meant when "dispersion" is invoked for nonbonded interactions occurring at distances within about 6 Å), and has been specifically recommended for transition metal containing systems; M06-L offered the best agreement of several tested functionals compared to large multireference calculations and several benchmark studies have confirmed its excellent accuracy in this respect.[19−25] Gradient-based minimization methods using the unrestricted formulizm were used for minimum energy geometry optimizations. Additionally, wave function stability tests were carried out to confirm the energetic minimum, and vibrational analyses were performed for each structure to ensure the absence of imaginary frequencies. Atomic spin densities and atomic charges derived from Mulliken population analyses were summarized. Gas-phase electron affinities and proton affinities are discussed and are interpreted with reference to those computed for models of similar size, charge, and chemical structure for which both experimental and computational data are already available[26−28] thus offering a means of calibrating gas-phase affinities against experimental data on proteins. In addition, all structures were calculated in solvent by employing the conductor-like polarizable continuum model (CPCM)[29] and a dielectric constant ε = 4 as implemented in Gaussian 09. As somewhat expected,[26−28] relative trends seen in proton and electron affinities in gas-phase calculations were conserved in the solvated models (including the reference states, which were for this purpose recalculated in solvent); these latter data are illustrated in Supporting Information. All structures in this study were visualized using the XYZViewer visualization program.[30]

RESULTS AND DISCUSSION

Table 1 illustrates the geometry optimization results of Fe(III)−H_2NOH. Table 2 lists all models investigated in this work, with absolute energies, key bond lengths, and Mulliken atomic spin densities and charges. Proton and electron affinities in the form of energy differences between various models are expressed in kcal/mol in Table 3, while Figure 2 summarizes the findings and provides explicit structures of the calculated species.

Table 1 reveals a low spin doublet ground state for Fe(III)−H_2NOH, with one spin unit on iron and an essentially neutral hydroxylamine ligand. The quartet and the sextet spin states, however, are considered energetically accessible at 4.6 and 1.6 kcal/mol higher than the ground state, respectively. The low spin state is utilized in all further calculations concerning the reactive intermediates.

$[Fe(III)−H_2NOH]^{1+}$ (structure **1**) would have the option of either losing one electron to yield $[Fe−H_2NOH]^{2+}$ (**2**) or

dx.doi.org/10.1021/jp507023a | J. Phys. Chem. B XXXX, XXX, XXX−XXX

Table 3. Proton and Electron Affinities (kcal/mol) for Putative Catalytic Intermediates in the 2-Electron 2-Proton Reaction of Fe(III)−H_2NOH to Fe(III)−HNO, Compared with Those Computed for Species of Similar Size and Charge

number	formal description	proton affinity	electron affinity
	Fe(II)-oxy, heme oxygenase [0]	252	36
	HRP Compound I [+1]		140
	protonated HRP Compound I [+2]		223
	protonated HRP Compound II [+1]		120
	unprotonated HRP Compound II [0]	264	
	Fe(III)−hydroxo, Hb/HRP [0]	253	
	Fe(III)−peroxo, Hb/HRP [-1]	358	
1	Fe(III)−H_2NOH [+1]		
2	Fe(IV)−H_2NOH [+2]		229
3	Fe(II)−HNOH [0]	267	
4	Fe(III)−HNOH [+1]	172	134
5	Fe(V)−H_2NOH [+3]		287
6	Fe(I)−HNO [-1]	353	
7	Fe(IV)−HNOH [+2]	96	211
8	Fe(II)−HNO [0]	236	17
9	Fe(III)−HNO [+1]	148	122

losing one proton to yield a $[Fe{-}HNOH]^0$ adduct (**3**). It can be noticed from Table 2 that (**2**) can best be described as $Fe(IV){-}H_2NOH^0$ which is evident from zero spin units on Fe and an essentially neutral H_2NOH ligand. Conversely, the atomic spin densities of 0.55 and 0.54 on Fe and HNOH, respectively, in (**3**) reveal an interesting electronic structure which can be described as a mixture between Fe(II)-HNOH$^\bullet$ and Fe(III)−$HNOH^-$—an instance of redox isomerism that is somehow analogous to the ferrous-superoxo/ferric-peroxo case of superoxide reductase, or the Fe(II)−O_2 vs Fe(III)−O_2— case of oxyhemoglobin; a better comparison would however be with the arguably isoelectronic species Fe(III)−OOH^-, ferric-hydroperoxo, whose redox isomer would be Fe(II)-OOH$^\bullet$, that is, ferrous iron bound to a neutral superoxide.[31] The N−O bond length in (**3**) is only 0.02 Å shorter than in the hydroxylamine adduct (**1**), suggesting still a strong contribution from the redox isomer with a still nonoxidized ligand. Table 3 shows that the gas-phase proton affinity of the $[Fe{-}HNOH]^0$ adduct (**3**) is 267 kcal/mol which is similar to the 264 kcal/mol computed for the Compound II of HRP (horseradish peroxidase) and of globins. For these Compound II species there is a debate that has placed the pK_a at values ranging from ~8.5 to 4.5 or even lower.[31] This suggests that the deprotonation of (**1**) to yield (**3**) may be feasible in a physiologically relevant pH range. Moreover, the already partial character of Fe(II) appears as a logical step forward in the reaction, by partly abstracting the first electron from the substrate, HA. By contrast, the alternative pathway, where the first step in the mechanism would involve formation of the Fe(IV) complex (**2**), may be argued to be unlikely: this is because the electron affinity for (**2**) (i.e., describing the opposite reaction to the desired one), at 229 kcal/mol, is even larger that the electron affinity of HRP Compound I, a species notable as one of the most potent oxidizers in biology. We then

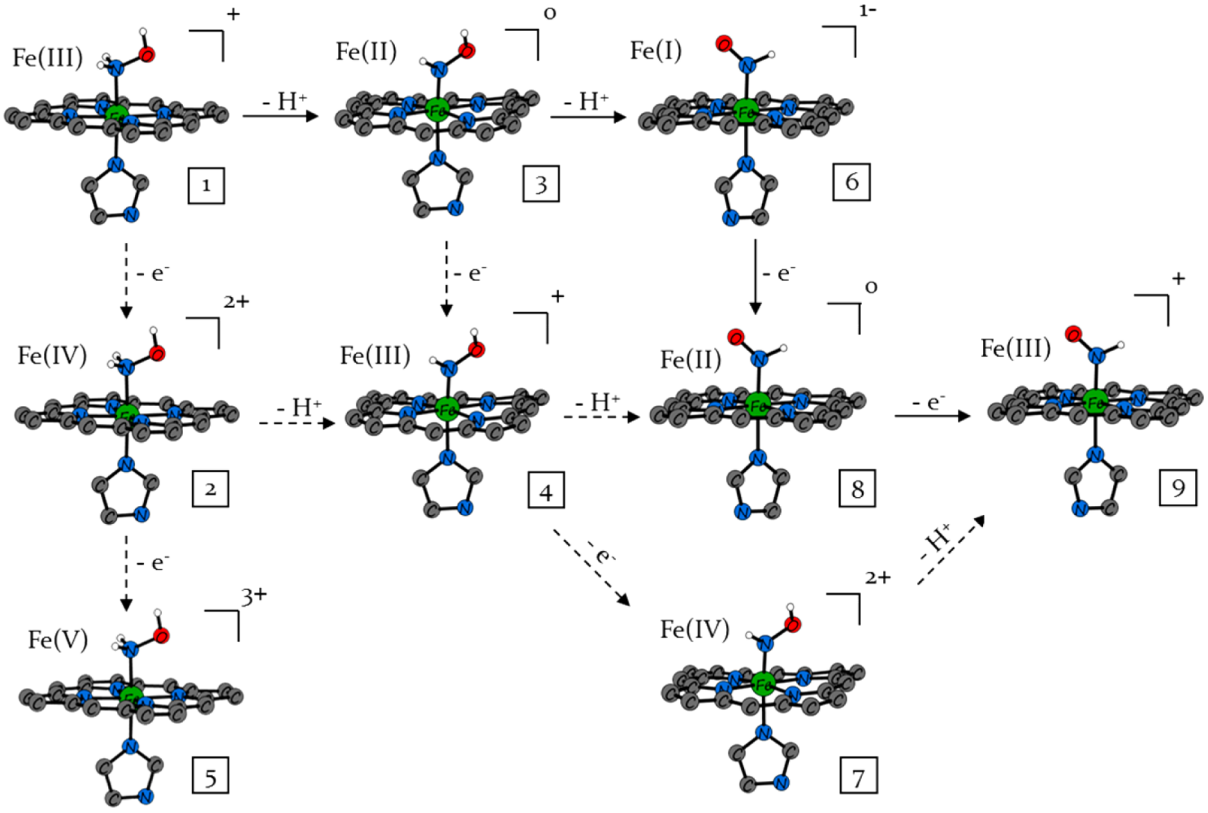

Figure 2. Proposed pathway for the 2-electron 2-proton transfer reaction of Fe(III)−H_2NOH to Fe(III)−HNO in HAO. Solid lines represent feasible pathways while dashed lines represent pathways that are highly unlikely to occur though not impossible. In each structure, hydrogen atoms of the porphine ring and the imidazole ligand are omitted for clarity.

dx.doi.org/10.1021/jp507023a | J. Phys. Chem. B XXXX, XXX, XXX−XXX

conclude that our proposed first step in the sequence of two-electron two-proton transformation of the iron-bound HA is a deprotonation event.

Species (**3**), that is, $[Fe(II)-HNOH^{\bullet} \leftrightarrow Fe(III)-HNOH^{-}]^{0}$, will then have the option of losing an electron to form $[Fe(III)-HNOH^{0}]^{1+}$ (**4**) or lose a proton to yield $[Fe-HNO]^{-}$ (**6**). Species (**4**) is found to retain a decidedly neutral NHOH ligand (cf. Table 2: 0.08 net charge, alongside an N−O bond length shorted by 0.06 Å compared the intact H_2N-OH ligand), suggesting a covalent bond formed by the unpaired d_z^2 electron of a low-spin Fe(III) and the NHOH radical, yielding a diamagnetic state. For species (**6**), several redox isomers may be proposed: $Fe(I)-HNO \leftrightarrow Fe(II)-HNO^{\bullet-} \leftrightarrow Fe(III)-HNO^{2-}$. The clear spin density on the ligand, of 0.53, in fact antiferromagnetically coupled to the −0.36 on the metal, is reminiscent of other six-coordinated formally Fe(I) complexes,[32] where redox isomerism was also noted.

The conversion of (**3**) into (**4**) appears unlikely, since the electron affinity of (**4**) is slightly larger than that computed for the known strong oxidant HRP Compound II—suggesting that, if anything, the back-reaction might be more reasonable. On the other hand, further deprotonation of (**3**) into (**6**) appears more reasonable: the proton affinity of (**6**) is slightly lower than that of histidine-ligated ferric-hydroperoxo complexes such as those in globins of HRP. The feasibility of such complexes as $Fe(III)-H_2O_2$ as transient unstable species has been discussed and is proposed to be relevant in the catalytic cycles of for example, heme oxygenases.[33]

We therefore propose that the second step in the sequence of two-electron two-proton transformation of the iron-bound HA is also a deprotonation event. The presence of the several hemes nearby the catalytic site (intriguingly, twice as many hemes are present per subunit as the number of electrons needed for one catalytic cycle) hints at a possible concerted process, where this second deprotonation is accompanied by electron transfer. Indeed, from this point onward the next two logical steps are two consecutive one-electron oxidations, from (**6**) to Fe(II)−HNO (**8**) and then to Fe(III)−HNO (**9**). Indeed, Table 3 shows that the electron affinity of (**8**) is relatively low, distinctly lower than the electron affinity of the oxy heme in hemoglobin—a species known to be itself relatively stable—which thus suggests the conversion of (**6**) to (**8**) is entirely feasible.

With the formation of (**8**), two protons and one electron have been transferred away from HA, of the total of two protons and two electrons proposed to entail the first part of the catalytic cycle, apparently leaving no choice about the next step, a final one-electron oxidation. Yet (**9**) does seem to feature a large proton affinity, close to that of HRP Compound II, suggesting that Fe(III)−HNO is less likely to be a distinct "station" in the catalytic cycles of HAO and that the reaction would rather proceed from (**8**) by deprotonation, possibly concerted to one-electron oxidation. These steps, leading from an HNO ligand to an NO ligand and then to nitrite, remain to be examined as a separate topic, especially in the context in which they have been approached computationally by other groups as well.[15] Figure 2 then summarizes the proposed sequence, out of the several possibilities examined, for the first two electrons and two protons in the HAO catalytic cycle.

The recently resolved 4N4O pdb crystal structure[32] reveals as a first detectable reaction intermediate a bent Fe−N−O moiety at an HAO-type active site. The authors ascribe this as a $[FeNO]^7$ center, because it was obtained by soaking the crystals with NH_2OH, but also because in experiments performed in solution they have shown that the reaction of the as-isolated (all-ferric) enzyme with hydroxylamine leads to a two-electron oxidation of the enzyme as ascertained by the UV−vis features of the hemes. The resolution of the crystal structure does not allow for protons to be observed directly. The authors also note, in the same structure, that the side-chains of an aspartate and of a histidine appear to be in hydrogen-bonding distance from the *oxygen* atom of the Fe-NO moiety. Interestingly, these two side-chains are close enough to each other to form a direct hydrogen bond between them, which would be quite expected of a His + Asp pair. Yet, they are both directed at the oxygen atom of the Fe-NO, suggesting an unprecedentedly strong interaction for a nitric oxide. $[FeNO]^7$ in general has been described as displaying significant nitroxyl character.[33] This may justify hydrogen bonding with the His in the 4N4O pdb crystal structure; nevertheless, one needs to note that the second nitrogen of the imidazole ring is already pointing toward a set of two carbonyl oxygens, in a position that can normally be reconciled precisely with a protonated nitrogen. In this context, it is further surprising that rather than being oriented toward the positively charged doubly protonated His, the Asp is pointing toward the negatively charged oxygen atom of the Fe−NO. This Asp orientation can be explained if the carboxylate is protonated, but such protonation appears unexpected when one considers the neighboring groups, unless we are trapped in an unstable reaction intermediate defined precisely by this temporary Asp protonation. An alternative interpretation might be that the NO ligand does in fact harbor some proton(s) on the distal atom. This can arise in two ways. One would be that in the crystal a hydroxylamine molecule may well have reduced the protein by two electrons, but that it was later replaced by a second hydroxylamine molecule. This, however, would imply either a protonated Asp (for which as stated above there is no further ground to argue), or, if the Asp is deprotonated and thus holding the hydroxylamine OH proton in a hydrogen bond, it would then mean that the His is doubly protonated. Since the active site is designed to abstract protons, not to donate them, such a situation may only be regarded as a possible reaction intermediate resulting after the extraction of protons from a previous HA molecule. A second possible explanation might be that there are two protons on the distal atom, and that each of these protons is held by one of the hydrogen bond acceptors—an anionic Asp and a neutral His; this would only be possible if the complex is $Fe-O(H)-NH_2$, a linkage isomer of the previously observed sole mode of binding of hydroxylamine to HAO or indeed to any hemes so far. Interestingly, the same enzyme hydrazine when bound to the active site heme does not form a hydrogen bond with the distal Asp.[32] The authors propose that the hydrazine structure in fact contains a diazene ligand, HN═NH. Either way, the distal atom in such a structure might be expected to be a weaker proton donor in a hydrogen bond compared to an OH group. Also, the stereochemistry of the hydrazine would favor the distal NH_2 protons to point downward in order to avoid an eclipsed conformation with respect to the iron-bound NH_2 group (likewise for diazene favoring a trans configuration), whereas hydroxylamine would feature less sterical constraints in this respect. One may further need to consider the fact that the space between the NO moiety and Tyr358 and the above-discussed His allows ample room for a solvent molecule to intervene and reorganize hydrogen-bonding patterns (especially as the Tyr358 phenolic oxygen is pointing toward the FeNO

dx.doi.org/10.1021/jp507023a | J. Phys. Chem. B XXXX, XXX, XXX−XXX

oxygen at a distance of 5 A, which may be reconciled with a water-mediated hydrogen-bonding network). Last but not least, while two acid−base residues appear in direct contact with the oxygen atom of the heme-bound HA in HAO, and a further tyrosine is also positioned for potentially assisting proton trafficking from the same oxygen atom, no such contacts are apparently present for taking up the protons of the iron-bound nitrogen atom of HA. These considerations reveal a need for follow-up studies on the mechanism of hydrazine reduction by HAO-type active sites, as well as further consideration of the possibility of linkage isomerism in HAO.

To summarize, while many studies have been reported focusing on the NO intermediates of HAO, reported here is the first attempt to investigate the 2-electron 2-proton reaction of Fe(III)−H_2NOH to Fe(III)−HNO, which constitutes the first series of steps in the catalytic cycle. The exact sequence by which electrons and protons are lost was investigated using density functional theory. Two subsequent protonation events were proposed to initiate the process, of which the second is proposed to be concerted with a one-electron oxidation. The final one-electron oxidation was further proposed to be concerted with a third deprotonation, suggesting that Fe(III)−HNO may not be an isolable intermediate in the HAO catalytic cycle. Subsequent studies should be aimed at the following steps in the catalytic cycle as well as on the influence of the lateral substituents of the heme (and especially of the Cys and Tyr cross-links), on the comparative study of hydrazine oxidation, on the proton delivery network in the distal site, and possibly, on linkage isomerism.

■ ASSOCIATED CONTENT

Supporting Information

Proton and electron affinities for putative catalytic intermediates, as well as for species of similar size and charge, as computed in solvent with a dielectric constant of 4. This material is available free of charge via the Internet at http://pubs.acs.org.

■ AUTHOR INFORMATION

Corresponding Author

*E-mail: rsilaghi@chem.ubbcluj.ro.

Notes

The authors declare no competing financial interest.

■ ACKNOWLEDGMENTS

Funding from the Romanian Ministry of Education and Research (Grant PCCE 488/2012) is gratefully acknowledged.

■ REFERENCES

(1) Terry, K. R.; Hooper, A. B. Hydroxylamine Oxidoreductase: A 20-Heme, 200000 Molecular Weight Cytochrome C with Unusual Denaturation Properties which Forms A 63000 Molecular Weight Monomer after Heme Removal. *Biochemistry* **1981**, *20*, 7026−7032.

(2) Igarashi, N.; Moriyama, H.; Fukuomori, Y.; Tanaka, N. The 2.8 Å Structure of Hydroxylamine Oxidoreductase from a Nitrifying Chemoautotrophic Bacterium, *Nitrosomonas Europaea*. *Nat. Struct. Biol.* **1997**, *4*, 276−284.

(3) Arciero, D. M.; Hooper, A. B. Hydroxylamine Oxidoreductase from *Nitrosomonas Europaea* Is a Multimer of an Octa−Heme Subunit. *J. Biol. Chem.* **1993**, *268*, 14645−14654.

(4) Arciero, D. M.; Hooper, A. B.; Cai, M.; Timkovich, R. Evidence for The Structure of The Active Site Heme P460 In Hydroxylamine Oxidoreductase of Nitrosomonas. *Biochemistry* **1993**, *32*, 9370−9378.

(5) Enemark, J. H.; Feltham, R. D. Principles of Structure, Bonding, and Reactivity for Metal Nitrosyl Complexes. *Coord. Chem. Rev.* **1974**, *13*, 339−406.

(6) Hooper, A. B.; Terry, K. R. Hydroxylamine Oxidoreductase of Nitrosomonas. Production of Nitric Oxide from Hydroxylamine. *Biochim. Biophys. Acta* **1979**, *571*, 12−20.

(7) Hooper, A. B.; Balny, C. Reaction of Oxygen with Hydroxylamine Oxidoreductase of Nitrosomonas: Fast Kinetics. *FEBS Lett.* **1982**, *144*, 299−303.

(8) Hendrich, M. P.; Upadhyay, A. K.; Riga, J.; Arciero, D. M.; Hooper, A. B. Spectroscopic Characterization of the NO adduct of Hydroxylamine Oxidoreductase. *Biochemistry* **2002**, *41*, 4603−4611.

(9) Cabail, M. Z.; Pacheco, A. A. Selective One-Electron Reduction of Nitrosomonas Europaea Hydroxylamine Oxidoreductase with Nitric Oxide. *Inorg. Chem.* **2003**, *42*, 270−272.

(10) Cabail, M. Z.; Kostera, J.; Pacheco, A. A. Laser Photoinitiated Nitrosylation of 3-Electron Reduced *Nm Europaea* Hydroxylamine Oxidoreductase: Kinetic and Thermodynamic Properties of the Nitrosylated Enzyme. *Inorg. Chem.* **2005**, *44*, 225−231.

(11) Walker, F. A. Nitric Oxide Interaction with Insect Nitrophorins and Thoughts on The Electron Configuration of The $\{FeNO\}^6$ Complex. *J. Inorg. Biochem.* **2005**, *99*, 216−236.

(12) Maes, E. M.; Roberts, S. A.; Weichsel, A.; Montfort, W. R. Ultrahigh Resolution Structures of Nitrophorin 4: Heme Distortion in Ferrous CO and NO Complexes. *Biochemistry* **2005**, *44*, 12690−12699.

(13) Roberts, S. A.; Weichsel, A.; Qiu, Y.; Shelnutt, J. A.; Walker, F. A.; Montfort, W. R. Ligand-Induced Heme Ruffling and Bent NO Geometry in Ultra-High-Resolution Structures of Nitrophorin 4. *Biochemistry* **2001**, *40*, 11327−11337.

(14) Senge, M. O. Exercises in Molecular Gymnastics—Bending, Stretching and Twisting Porphyrins. *Chem. Commun.* **2006**, 243−256.

(15) Fernandez, M. L.; Estrin, D. A.; Bari, S. E. Theoretical Insight into The Hydroxylamine Oxidoreductase Mechanism. *J. Inorg. Biochem.* **2008**, *102*, 1523−1530.

(16) Frisch, M. J.; Trucks, G. W.; Schlegel, H. B.; Scuseria, G. E.; Robb, M. A.; Cheeseman, J. R.; Scalmani, G.; Barone, V.; Mennucci, B.; Petersson, G. A.; Nakatsuji, H.; Caricato, M.; Li, X.; Hratchian, H. P.; Izmaylov, A. F.; Bloino, J.; Zheng, G.; Sonnenberg, J. L.; Hada, M.; Ehara, M.; Toyota, K.; Fukuda, R.; Hasegawa, J.; Ishida, M.; Nakajima, T.; Honda, Y.; Kitao, O.; Nakai, H.; Vreven, T.; Montgomery, J. A., Jr.; Peralta, J. E.; Ogliaro, F.; Bearpark, M.; Heyd, J. J.; Brothers, E.; Kudin, K. N.; Staroverov, V. N.; Kobayashi, R.; Normand, J.; Raghavachari, K.; Rendell, A.; Burant, J. C.; Iyengar, S. S.; Tomasi, J.; Cossi, M.; Rega, N.; Millam, J. M.; Klene, M.; Knox, J. E.; Cross, J. B.; Bakken, V.; Adamo, C.; Jaramillo, J.; Gomperts, R.; Stratmann, R. E.; Yazyev, O.; Austin, A. J.; Cammi, R.; Pomelli, C.; Ochterski, J. W.; Martin, R. L.; Morokuma, K.; Zakrzewski, V. G.; Voth, G. A.; Salvador, P.; Dannenberg, J. J.; Dapprich, S.; Daniels, A. D.; Farkas, O.; Foresman, J. B.; Ortiz, J. V.; Cioslowski, J.; Fox, D. J. Gaussian 09, revision A.01; Gaussian, Inc.: Wallingford, CT, 2009.

(17) Dennington, R.; Keith, T.; Millam, J. *GaussView*, version 5; Semichem Inc.: Shawnee Mission KS, 2009.

(18) Zhao, Y.; Truhlar, D. G. A New Local Density Functional for Main-Group Thermochemistry, Transition Metal Bonding, Thermochemical Kinetics, And Noncovalent Interactions. *J. Chem. Phys.* **2006**, *125*, 194101.

(19) Cramer, C. J.; Gour, J. R.; Kinal, A.; Wtoch, M.; Piecuch, P.; Shahi, A. R. M.; Gagliardi, L. Stereoelectronic Effects on Molecular Geometries and State-Energy Splittings of Ligated Monocopper Dioxygen Complexes. *J. Phys. Chem. A* **2008**, *112*, 3754−3767.

(20) Zheng, J.; Zhao, Y.; Truhlar, D. G. Representative Benchmark Suites for Barrier Heights of Diverse Reaction Types and Assessment of Electronic Structure Methods for Thermochemical Kinetics. *J. Chem. Theory. Comput.* **2007**, *3*, 569−582.

(21) Torker, S.; Merki, D.; Chen, P. Gas-Phase Thermochemistry of Ruthenium Carbene Metathesis Catalysts. *J. Am. Chem. Soc.* **2008**, *130*, 4808−4814.

(22) Zhao, Y.; Truhlar, D. G. The M06 Suite of Density Functionals for Main Group Thermochemistry, Thermochemical Kinetics, Noncovalent Interactions, Excited States, and Transition Elements: Two New Functionals and Systematic Testing of Four M06-Class Functionals and 12 Other Functionals. *Theor. Chem. Acc.* **2008**, *120*, 215−241.
(23) Zhao, Y.; Truhlar, D. G. Density Functionals with Broad Applicability in Chemistry. *Acc. Chem. Res.* **2008**, *41*, 157−167.
(24) Korth, M.; Grimme, S. "Mindless" DFT Benchmarking. *J. Chem. Theory Comput.* **2009**, *5*, 993−1003.
(25) Zhao, Y.; Truhlar, D. G. Benchmark Energetic Data in a Model System for Grubbs II Metathesis Catalysis and Their Use for the Development, Assessment, and Validation of Electronic Structure Methods. *J. Chem. Theory Comput.* **2009**, *5*, 324−333.
(26) Silaghi-Dumitrescu, R.; Silaghi-Dumitrescu, I. Hemes Revisited by Density Functional Approaches. 1. The Axial Ligand and The Dioxygen-Peroxo Chemistry. *Rev. Roum. Chim.* **2004**, 3−*4*, 257−268.
(27) Silaghi Dumitrescu, R.; Cooper, C. E. Transient Species Involved in Catalytic Dioxygen/Peroxide Activation by Hemoproteins: Possible Involvement of Protonated Compound I Species. *Dalton Trans.* **2005**, 3477−3482.
(28) Silaghi Dumitrescu, R.; Reeder, B. J.; Nicholls, P.; Cooper, C. E.; Wilson, M. T. Ferryl Haem Protonation Gates Peroxidatic Reactivity in Globins. *Biochem. J.* **2007**, *403*, 391−395.
(29) Cossi, M.; Rega, N.; Scalmani, G.; Barone, V. Energies, Structures, and Electronic Properties of Molecules in Solution with the C-PCM Solvation Model. *J. Comput. Chem.* **2003**, *24*, 669−81.
(30) De Marothy, S. *XYZViewer a Software for Molecular Visualization and Simple Property Calculations*; Stockholm University: Stockholm, Sweden, 2011.
(31) Silaghi-Dumitrescu, R. Redox Activation of Small Molecules at Biological Metal Centers. *Struct. Bond.* **2013**, *150*, 97−118.
(32) Maalcke, W. J.; Dietl, A.; Marritt, S. J.; Butt, J. N.; Jetten, M. S.; Keltjens, J. T.; Barends, T. R.; Kartal, B. Structural Basis of Biological NO Generation by Octaheme Oxidoreductases. *J. Biol. Chem.* **2014**, *289*, 1228−1242.
(33) Silaghi-Dumitrescu, R.; Makarov, S. V. A Computational Analysis of Electromerism in Hemoprotein Fe(I) Models. *J. Biol. Inorg. Chem.* **2010**, *15*, 977−986.